

## ORIGINAL ARTICLE

## The homeoprotein DLX3 and tumor suppressor p53 co-regulate cell cycle progression and squamous tumor growth

E Palazzo<sup>1,4</sup>, M Kellett<sup>1,4</sup>, C Cataisson<sup>2</sup>, A Gormley<sup>1</sup>, PW Bible<sup>1</sup>, V Pietroni<sup>1</sup>, N Radoja<sup>1</sup>, J Hwang<sup>1</sup>, M Blumenberg<sup>3</sup>, SH Yuspa<sup>2</sup> and MI Morasso<sup>1</sup>

Epidermal homeostasis depends on the coordinated control of keratinocyte cell cycle. Differentiation and the alteration of this balance can result in neoplastic development. Here we report on a novel DLX3-dependent network that constrains epidermal hyperplasia and squamous tumorigenesis. By integrating genetic and transcriptomic approaches, we demonstrate that DLX3 operates through a p53-regulated network. DLX3 and p53 physically interact on the p21 promoter to enhance p21 expression. Elevating DLX3 in keratinocytes produces a G1-S blockade associated with p53 signature transcriptional profiles. In contrast, DLX3 loss promotes a mitogenic phenotype associated with constitutive activation of ERK. DLX3 expression is lost in human skin cancers and is extinguished during progression of experimentally induced mouse squamous cell carcinoma (SCC). Reinstatement of DLX3 function is sufficient to attenuate the migration of SCC cells, leading to decreased wound closure. Our data establish the DLX3–p53 interplay as a major regulatory axis in epidermal differentiation and suggest that DLX3 is a modulator of skin carcinogenesis.

*Oncogene* (2016) 35, 3114–3124; doi:10.1038/onc.2015.380; published online 2 November 2015

## INTRODUCTION

Skin cancer is the most common form of all cancers, with cutaneous squamous cell carcinoma (SCC) comprising ~20% of skin malignancies.<sup>1,2</sup> A wide variety of skin cancers such as basal cell carcinomas, SCC and melanomas harbor mutations in the tumor suppressor gene *p53*.<sup>3,4</sup> Frequently acquired mutations in RAS or p53 lead to altered responses to growth factors, perturbing the balance between keratinocyte proliferation and differentiation that is crucial to prevent neoplastic transformation.<sup>2,5</sup>

During epidermal differentiation, keratinocytes acquire a specific gene expression profile that includes cell cycle inhibitors and tumor suppressor genes.<sup>6</sup> The expression of the cyclin-dependent kinase inhibitor p21 during growth arrest is controlled by the tumor suppressor p53 and the activation of p53 itself, within its role as a caretaker gene in regulating cell cycle progression.<sup>7,8</sup>

An important p53 family member with essential roles in epidermal homeostasis is the transcription factor p63.<sup>9</sup> The *p63* gene (TP63) encodes for multiple isoform products of alternate promoters ( $\Delta N$  and TA) and carboxy-terminal ends ( $\alpha$ ,  $\beta$ ,  $\delta$ ,  $\epsilon$ ,  $\gamma$  and  $\zeta$ ).<sup>9–11</sup> Owing to the complexity of p63 isoforms, it has been challenging to determine their exact roles in terms of enhancing or blocking cell proliferation. Although rarely deleted or mutated, TP63 is frequently deregulated in human cancers.<sup>12,13</sup> In cutaneous SCC, high levels of p63 is used as a diagnostic marker<sup>14</sup> and recent characterization of isoform-specific deletions has highlighted the tumor suppressive functions or oncogenic function of the TA versus the  $\Delta Np63$  isoforms.<sup>11,15–17</sup>

Homeobox transcription factors have critical roles in gene regulatory networks that control developmental homeostasis,<sup>18</sup> with their expression being also dysregulated in cancer.<sup>19</sup> It has been shown that homeoproteins can act as drivers of tumor

initiation and progression through regulation of proliferation, migration and survival pathways.<sup>20</sup> The DLX3 homeodomain regulator is expressed during calcium (Ca<sup>++</sup>)-dependent epidermal differentiation process<sup>21,22</sup> and epidermal-specific deletion of DLX3 leads to epidermal hyperplasia, accompanied by barrier disruption and associated development of an inflammatory response.<sup>23</sup> DLX3 mutations have been associated with tricho-dento osseous, an ectodermal dysplasia<sup>10</sup> characterized by abnormalities in hair, teeth and bone.<sup>24</sup> DLX3 is a target of p63 during ectodermal development and is involved in a regulatory feedback loop with p63, which is crucial for the maintenance of the stratified epithelia.<sup>25,26</sup> Mutations in p63 are also associated with human hereditary syndromes.<sup>27</sup>

The functional interplay between p53, p63 and transcription factors in the regulation of keratinocyte differentiation has been recently highlighted for Runx1.<sup>28</sup> Here we show that by co-regulation with p53, DLX3 affects p53 downstream targets to modulate cell cycle exit in the skin and acts as a proliferative brake. On the other hand, loss of DLX3 is conducive to a pre-neoplastic state. Consistent with this model, DLX3 is lost in human and experimentally induced murine SCCs, supporting a function of DLX3 in the context of cutaneous tumorigenesis.

## RESULTS

## DLX3 promotes cell cycle arrest

We assessed the impact of DLX3 transcriptional function by transducing proliferative human epidermal keratinocytes with a retroviral vector expressing DLX3 (pHAN-DLX3/Flag) (Figure 1). DLX3 expression induced morphological changes characteristic of keratinocyte differentiation (Figure 1a). Gene ontology analysis of differentially regulated transcripts showed that exogenous DLX3

<sup>1</sup>Laboratory of Skin Biology, NIAMS, NIH, Bethesda, MD, USA; <sup>2</sup>Laboratory of Cancer Biology and Genetics, NCI, NIH, Bethesda, MD, USA and <sup>3</sup>Department of Dermatology, New York University, New York, NY, USA. Correspondence: Dr MI Morasso, Laboratory of Skin Biology, NIAMS, NIH, Building 50, Room 1523, Bethesda, MD 20892, USA. E-mail: morasso@nih.gov

<sup>4</sup>These authors contributed equally to this work.

Received 3 April 2015; revised 10 August 2015; accepted 4 September 2015; published online 2 November 2015

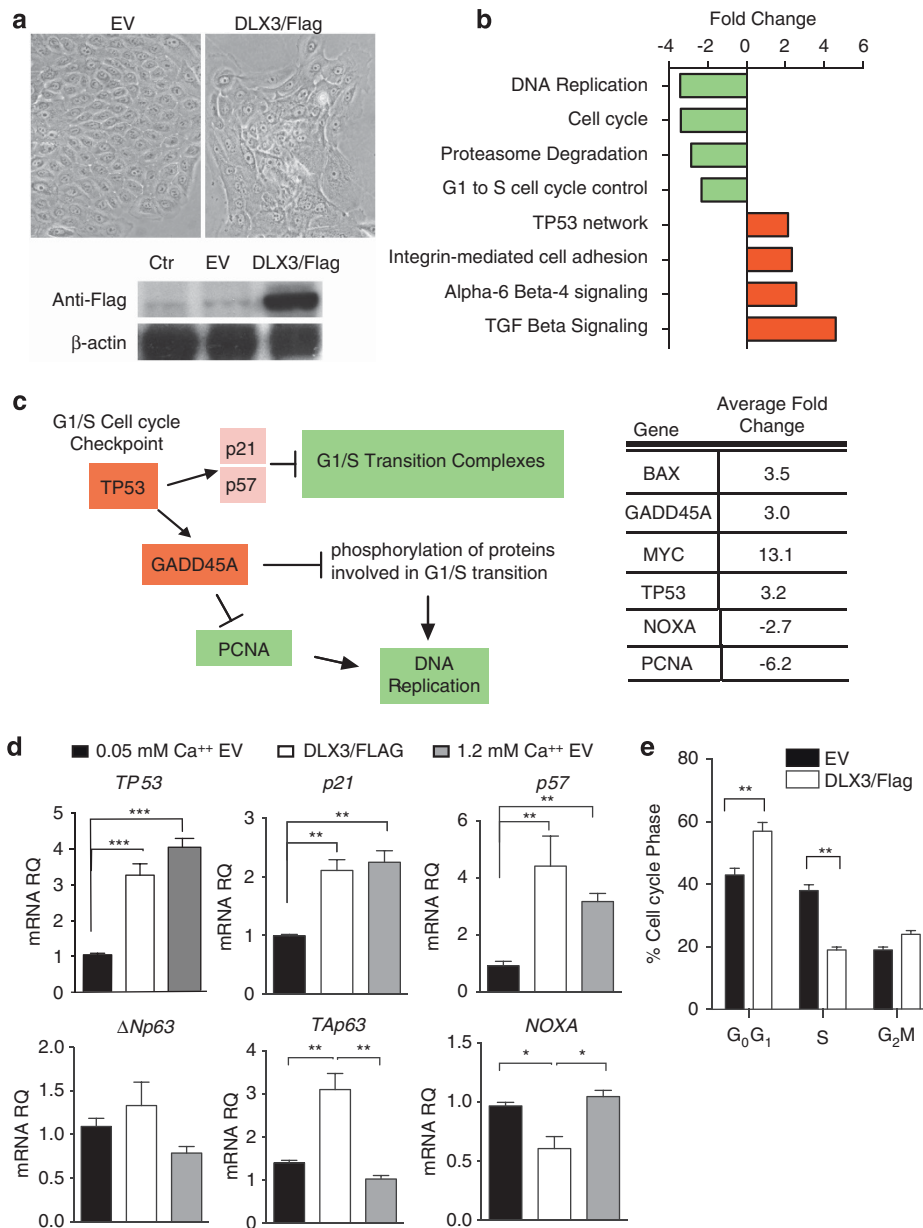


**Figure 1.** DLX3-dependent p53 signaling network activation drives cell cycle exit and differentiation. **(a)** Upper panel: NHEK transduced with empty vector (EV) or pHan-DLX3/Flag (DLX3/Flag)-expressing vectors in proliferating media (0.05 mM Ca<sup>++</sup>). Cell morphology was assessed 24 h post infection. Lower panel: western blot analysis with anti-Flag or β-actin antibodies. **(b)** Top significant biological pathways in microarray data of DLX3-transduced keratinocytes ranked by fold change average and determined by Wikipathways analysis. **(c)** Left panel: a subset of the G1 to S cell cycle control pathway determined by Wikipathways database overlaid with DLX3-transduced keratinocyte expression profile. Red and green boxes represent up- and downregulated genes, respectively. Right panel: p53 target gene fold change in DLX3-transduced keratinocytes (fold change > ±2; *P* < 0.05). **(d)** Bar graphs showing relative expression level of TP53, p21, p57, ΔNp63, TAp63 and NOXA in DLX3-transduced keratinocytes. The results are shown as mean ± s.d. of three independent experiments. \**P* < 0.05, \*\**P* < 0.001 and \*\*\**P* < 0.01. **(e)** Propidium iodide staining of EV and DLX3-transduced keratinocytes (mean ± s.d.; \*\**P* < 0.05).

expression promoted the dysregulation of genes involved in DNA replication, cell cycle, G1 to S cell cycle control, as well as p53 network and transforming growth factor-β signaling pathways (Figure 1b and Supplementary Table 1). Of particular relevance were the increased levels of TP53 and cyclin-dependent kinase inhibitors p21 and p57 transcript, as well as those of proteins involved in the formation of the G<sub>1</sub>/S transition complexes (Figure 1c left and right panels; Supplementary Tables 2 and 3). The cyclin-dependent kinase inhibitors p21 and p57 share a wide range of cyclin/cdk targets to modulate G1 phase progression.<sup>29</sup>

Studies of p21 null mouse keratinocytes support that p21 is required for initial commitment of keratinocytes to differentiate.<sup>7,30</sup> DLX3-transduced keratinocytes showed high levels of BAX and GADD45, which are critical factors for cell cycle arrest in differentiating cells (Figure 1c right panel and Supplementary Table 3).<sup>31</sup> We also found significant upregulation of MYC, a well-established effector of epidermal differentiation,<sup>32</sup> in contrast with specific downregulation of proliferation markers such as proliferating cell nuclear antigen (PCNA) (Figure 1c, right panel). Alteration in multiple networks were filtered by focusing

on factors of known function in cell cycle control. The down-regulation of proteins involved in DNA replication are also consequences of DLX3-regulated functions (Supplementary Tables 2 and 3). Significant DLX3-dependent upregulation of TP53, p21, p57 and TAp63 was verified by quantitative PCR (Figure 1d).  $\Delta$ Np63 and TAp63 have essential roles in epidermal differentiation, being associated with proliferation or cell cycle break/apoptosis, respectively.<sup>9,33–35</sup> A role for TAp63 in the transcriptional control of keratinocyte differentiation has been recently reported.<sup>36</sup> Although the expression of  $\Delta$ Np63 was not significantly modulated in DLX3-overexpressing human keratinocytes, we found significant modulation of a p63 target, NOXA.<sup>37</sup> Our findings support a model in which DLX3 function is critical for cell cycle regulation and triggering terminal differentiation.

Thus, our results indicate that DLX3 expression in proliferating keratinocytes globally drives cell cycle block and a switch to a

suprabasal profile (Supplementary Table 4), and promotes the upregulation of p53 target genes.<sup>38</sup> These data were corroborated by results from a PCR with reverse transcription profiler array (Supplementary Figure 1). Cytofluorimetric analysis confirmed the increased accumulation of cells in G<sub>0</sub>G<sub>1</sub> and a 50% decrease in cells in S phase (Figure 1e).

#### DLX3 and p53 co-regulate p53 target, p21

Given the DLX3-dependent modulation of p53-regulated networks in skin, we investigated the transcriptional regulation and expression of the well-known p53 targets utilizing RNA interference experiments. Reduced expression of p53 resulted in a significantly decreased upregulation of p21 and epidermal differentiation markers such as KRT10 (Figure 2a). Interestingly, the broader impact of p53 silencing was also reflected in the

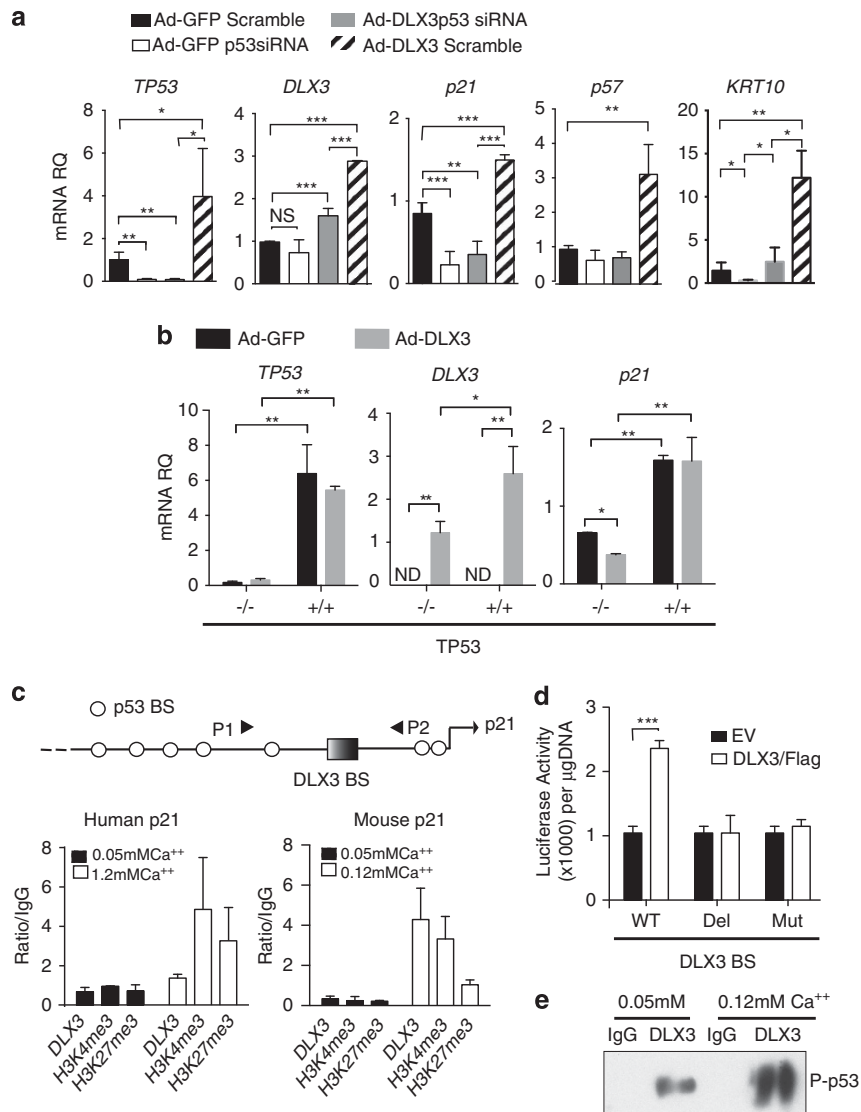


**Figure 2.** DLX3 promotes p53-dependent p21 transcription. **(a)** Relative expression levels of TP53, DLX3, p21, p57 and KRT10 in keratinocytes transfected with scramble or p53 siRNA and transduced with Ad-GFP or Ad-GFP-DLX3 (mean  $\pm$  s.d.; \* $P$  < 0.05, \*\* $P$  < 0.01 and \*\*\* $P$  < 0.001). **(b)** Relative expression levels of TP53, DLX3 and p21 in TP53 null HCT116 cells and TP53 WT HCT116 cells transfected with Ad-GFP or Ad-GFP-DLX3 (mean  $\pm$  s.d.; \* $P$  < 0.05 and \*\* $P$  < 0.001). **(c)** Top panel: p53 and DLX3 consensus sites on the p21 promoter. Bottom panel: ChIP assay with DLX3, H3K4me3 and H3K27me3 antibodies showing specific binding on p21 promoter. IgG antibody was used as control. **(d)** Bar graph showing p21 promoter activity induced by DLX3 measured by luciferase assay. Normal human keratinocytes were co-transfected with p21 promoter constructs (WT, deleted (Del) or mutated (Mut) DLX3-binding site), and pHan-DLX3/Flag or pHan-EV. **(e)** Western blot showing P-p53 pull down by DLX3 antibody of primary keratinocyte cell lysates in proliferating and differentiating media.



significantly reduced DLX3, p21 and p57 expression in DLX3-transduced cells. These results were corroborated using p53-knockout HCT116 cells,<sup>39</sup> where p21 expression and endogenous DLX3 transcription were not induced by DLX3 in the absence of p53 function (Figure 2b).

The role of p21 in the epidermal differentiation process and its transcriptional regulation by p53 has been reported.<sup>7,30,40</sup> Analysis of the p21 promoter region determined the presence of a potential binding site for DLX3 (Figure 2c, top panel; -2475 to -2457 in mouse and -2261 to -2242 in human). Pull-down assays with anti-H3K4me3 or anti-H3K27me3 antibodies confirmed that this region was bound by DLX3 and was transcriptionally active in differentiating keratinocytes (Figure 2c, bottom panel). Luciferase assays using the p21 promoter containing a wild-type (WT), deleted or mutated DLX3-binding site (Figure 2d) as well as electromobility shift assays with anti-DLX3 antibody (Supplementary Figure 2) supported the functional relevance of DLX3 binding to the p21 promoter during Ca<sup>++</sup>-induced differentiation. This region of the p21 promoter also contained well-established conserved p53-binding sites (Figure 2c),<sup>40</sup> raising the possibility of the formation of a transcriptional complex necessary to regulate p21 transcription. We confirmed a specific, physical interaction between DLX3 and phosphorylated p53 on the p21 promoter that is enhanced in differentiating media (Figure 2e). These data highlight the role of DLX3 in the regulation of p21 gene transcription during differentiation. Furthermore, the association of DLX3 with p53 supports an essential transcriptional modulation activity within p53 network pathways in keratinocytes.

DLX3 expression is extinguished in skin cancer models

We next investigated a possible contribution of DLX3 to cutaneous tumorigenesis. The expression levels of DLX3 were monitored during tumor progression in the two-stage mouse model of skin cancer.<sup>41</sup> We show the extinction of DLX3 expression at both mRNA and protein levels as skin papillomas progress from low risk to high risk for conversion to SCCs (Figure 3). Selective ablation is noted in tumor areas expressing KRT13, a marker of progression from benign to malignant stage<sup>41</sup> (Figure 3c).

The strong association between DLX3 extinction and skin tumor progression prompted us to test the impact of DLX3 loss in keratinocytes transduced with v-ras<sup>Ha</sup> as an experimental cell system. Transduction of normal keratinocytes with an oncogenic RAS allele is sufficient to initiate skin carcinogenesis.<sup>42</sup> We found that the absence of DLX3 function correlates with a significantly lower expression of p21, p57 and p53 transcripts when compared with WT cells, independent of v-ras<sup>Ha</sup> (Figure 4a). Interestingly, DLX3cKO cells had higher levels of ΔNp63, supporting a function for DLX3 in the regulation of ΔNp63α levels, a mechanism that may contribute to reduce the abundance of ΔNp63α during differentiation of stratified epithelia.<sup>25</sup> The lower levels of ΔNp63 and the higher level of the TAp63 target p57 in v-ras-keratinocytes may potentially be due to the oncogene-induced replicative senescence.<sup>43,44</sup>

Although v-ras<sup>Ha</sup> transduction reduced Krt10 transcription and abolished protein expression in keratinocytes (Supplementary Figure 3a and Figure 4b), DLX3cKO cells display a profile characterized by lack of keratin 10 expression in the absence of v-ras transduction. Analysis of the RAS-MAPK pathway in DLX3cKO

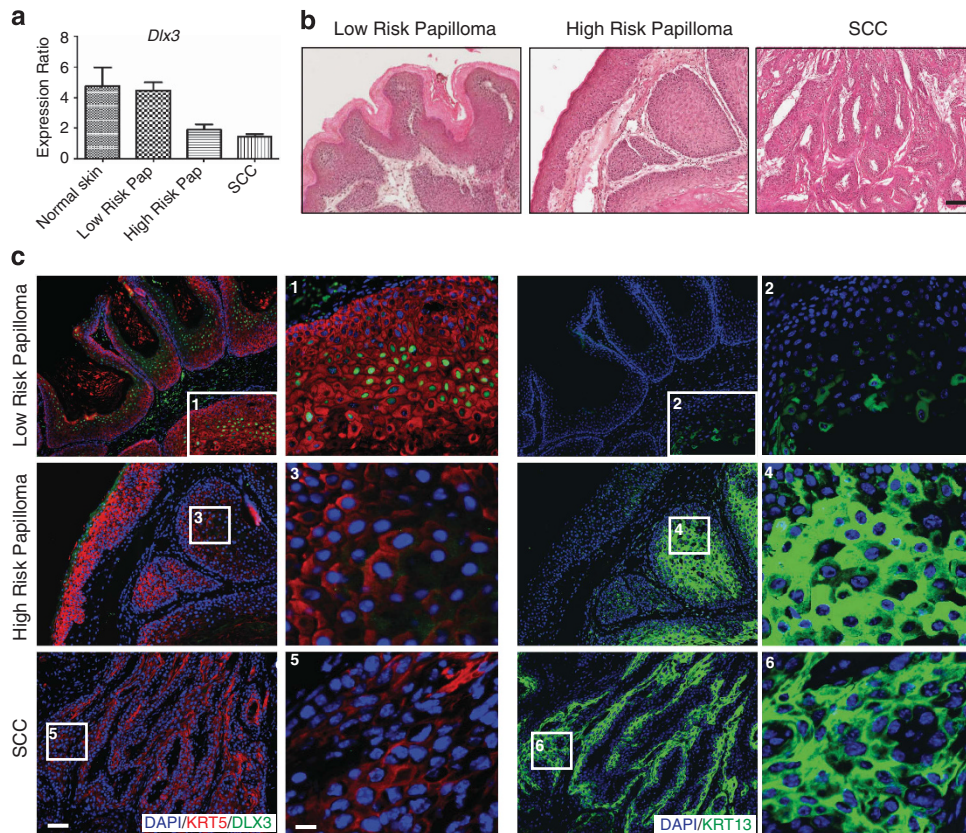


**Figure 3.** DLX3 expression is lost in mouse skin carcinogenesis model. **(a)** DLX3 expression level by microarray data analysis of normal, low- and high-risk papilloma and SCC lesions and **(b)** hematoxylin and eosin, and **(c)** immunohistochemical staining with antibodies against KRT5, DLX3 and KRT13 of (1 and 2) low-risk papilloma (3 and 4) high-risk papilloma and (5 and 6) SCC. Scale bar, 20 μm.

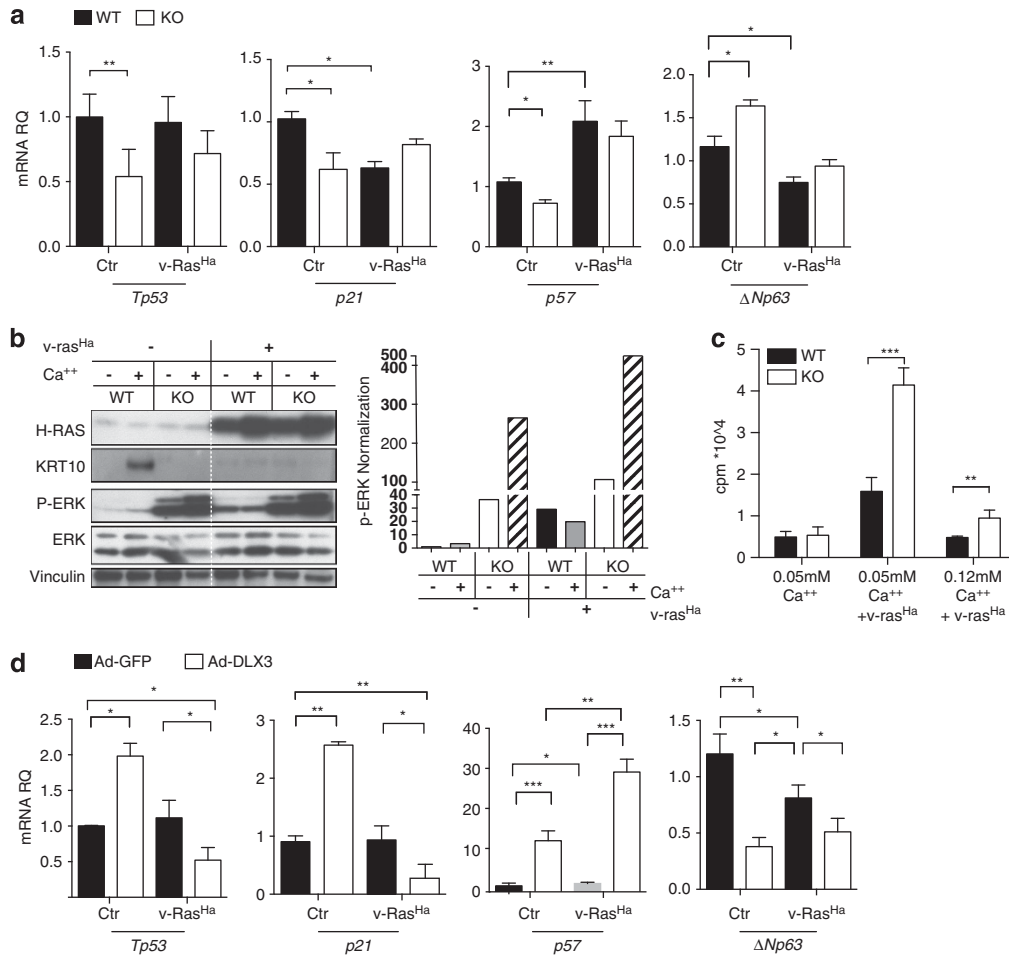


**Figure 4.** DLX3 loss promotes a mitogenic phenotype associated with constitutive activation of ERK. **(a)** Upper panel: relative expression levels of *Tp53*, *p21*, *p57* and  $\Delta Np63$  in WT and DLX3cKO keratinocytes transduced with v-ras<sup>Ha</sup>. **(b)** Western blot analysis utilizing H-RAS, KRT10, ERK, phospho-ERK and Vinculin antibodies in proliferative (0.05 mM Ca<sup>++</sup>) and differentiating (0.12 mM Ca<sup>++</sup>) media. Total ERK vs Phospho-ERK ratio was normalized to Vinculin expression. **(c)** Cell proliferation assessed by 3H-thymidine in proliferating or differentiating media. **(d)** Relative expression levels of *Tp53*, *p21*, *p57* and  $\Delta Np63$  from ras-transformed keratinocytes infected with Ad-GFP or Ad-DLX3 (mean  $\pm$  s.d.; \**P* < 0.05, \*\**P* < 0.01 and \*\*\**P* < 0.001).

keratinocytes showed that the loss of DLX3 in cultured keratinocytes was associated with the activation of ERK, even in the absence of v-ras<sup>Ha</sup> (Figure 4b). Proliferation was markedly increased, and growth arrest in response to Ca<sup>++</sup> was impeded in v-ras<sup>Ha</sup>-transduced DLX3cKO keratinocytes (Figure 4c). These results also support the inability of v-ras<sup>Ha</sup> keratinocytes to differentiate in the absence of DLX3.

Exogenous DLX3 significantly increased p57 expression in v-ras<sup>Ha</sup> keratinocytes (Figure 4d). On the other hand, while exogenous DLX3 did not restore the expression of Krt10 (Supplementary Figure 3c) it significantly modified p21, p53 or  $\Delta Np63$  expression in v-ras<sup>Ha</sup> keratinocytes, indicating a selective influence of DLX3 on v-ras<sup>Ha</sup> mediated transformation (Figure 4d). This indicates that DLX3 may induce cell cycle exit in ras-transformed keratinocytes through a p57-dependent pathway.

Interestingly, the expression of Cxcl1, a CXCR2 ligand essential for RAS-mediated tumor formation<sup>45</sup> was significantly higher in DLX3cKO v-ras<sup>Ha</sup> keratinocytes when compared with WT v-ras<sup>Ha</sup> keratinocytes (Supplementary Figure 3a). In contrast, exogenous expression of DLX3 in v-ras<sup>Ha</sup>-transduced keratinocytes reduced to nontransformed levels the release of CXCL1 and IL1 $\alpha$  that is critical for transformation of keratinocytes by v-ras<sup>Ha</sup> (Supplementary Figure 3b). Altogether, these results support that the loss of DLX3 leads to a mitogenic phenotype conducive to a proneoplastic state.

DLX3 expression is lost in human SCC as a function of RAS mutation

Our data highlight the correlation of DLX3 function and skin cancer progression, and that keratinocytes without DLX3 have characteristics of initiated cells. We further assessed the expression of DLX3 by immunohistochemical analysis of human skin carcinoma tissue microarrays containing sections of SCC and metastatic adenocarcinoma lesions. DLX3 expression was lost in all tumor stages, from well or moderately differentiated SCC (grade I and II) to metastatic poorly differentiated adenocarcinoma (grade III) and undifferentiated carcinoma samples (grade IV) (Biomax Tissue Array; SK208, US Biomax Inc., Rockville, MD, USA) (Figure 5a). All of these skin lesions strongly express the malignancy marker KRT13 (Supplementary Figure 4). Examination of published human transcriptome data sets (Oncomine, www.oncomine.org) showed that DLX3 mRNA levels were down-regulated in a cohort of head and neck SCC (HNSCC) lesions from oral mucosa (fold change: -2.310; *P*-value: 5.53E-11; Figure 5b). These lesions display decreased expression of TP53 and KRT1, and increased expression of TP63 (fold change: -1.892; *P*-value = 2.10E-11; fold change: -5.895; *P*-value = 1.78E-16; fold change: 1.238; *P*-value = 2.68E-4, respectively; Figure 5b). In the same data sets, a significant negative fold change for DLX3 was found in melanoma (fold change: -10.453; *P*-value: 3.24E-6),

colorectal (fold change:  $-3.249$ ;  $P$ -value:  $4.61E-16$ ) and breast cancer (fold change:  $-2.524$ ;  $P$ -value:  $1.47E-6$ ) when compared with normal tissue. DLX3 expression also exhibited a negative correlation with the increased level of tumor malignancy in head and neck SCC tumors from The Cancer Genome Atlas studies (TCGA; <http://cancergenome.nih.gov>) ( $P$ -value:  $9.756E-10$ ; Figure 5c). Thus, comparative analysis of expression data highlights the association between loss of DLX3 expression and the progression of SCCs.

**Reinstatement of DLX3 in SCC cell lines alters cell cycle and differentiation**

As DLX3 expression is undetectable in human SCCs, we examined the levels of DLX3 expression in SCC lines and confirmed that it is abolished in SCC13 and SCC9 (Figure 6a). We hypothesized that the reinstatement of DLX3 into SCC cell lines would impact cell cycle. To analyze the effect of DLX3 function in SCC9 and SCC13 lines, we utilized a scratch assay to study migration upon infection with Ad-GFP or Ad-DLX3. We determined that wound closure occurred at a delayed rate upon addition of Ad-DLX3 in both

SCC13 and SCC9 (Figures 6b and c), and could be morphologically observed by 18 h post infection.

To investigate the transcriptional programs underlying the reduced wound closure upon DLX3 restoration, we performed transcriptomic profiling of SCC13 infected with Ad-GFP or Ad-DLX3 at 18, 24, 36 or 48 h post infection. An Ingenuity Pathway Analysis (IPA; [www.ingenuity.com](http://www.ingenuity.com)) of the genes at 48 h (fold change  $>2$  and  $<-2$ ) revealed a negative activation Z-score for genes related to cell movement, cancer, growth and cell cycle (Figure 6d and Supplementary Table 5). At 48 h post infection we show that, while TP53 was unaffected,<sup>46</sup> specific transcriptional targets related to the G<sub>1</sub>/S phase were differentially regulated (Supplementary Table 6). Isoforms of the *CDKN2a* gene, p16INK4A and p14ARF were upregulated (6.5- and 8.8-fold, respectively), with downstream targets regulated to promote inhibition of the G1 to S transition (Figure 6e).

We then sought to understand the global transcriptional changes of the differentially regulated genes at 18, 24, 36 and 48 h post infection. A heat map of hierarchically clustered fold changes reveal a trend toward upregulation of genes involved in negative regulation of the cell cycle, signaling and cell adhesion in

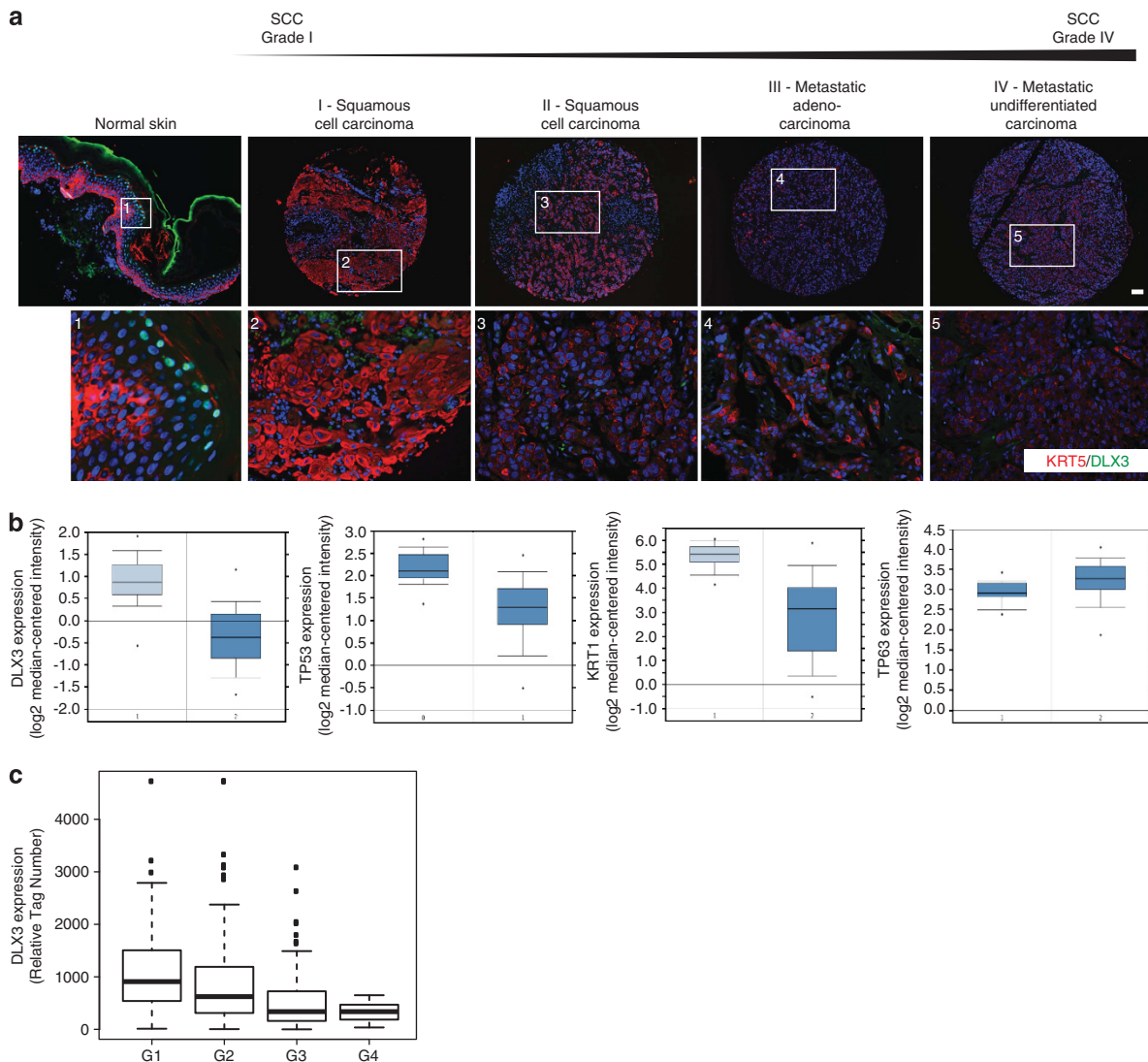
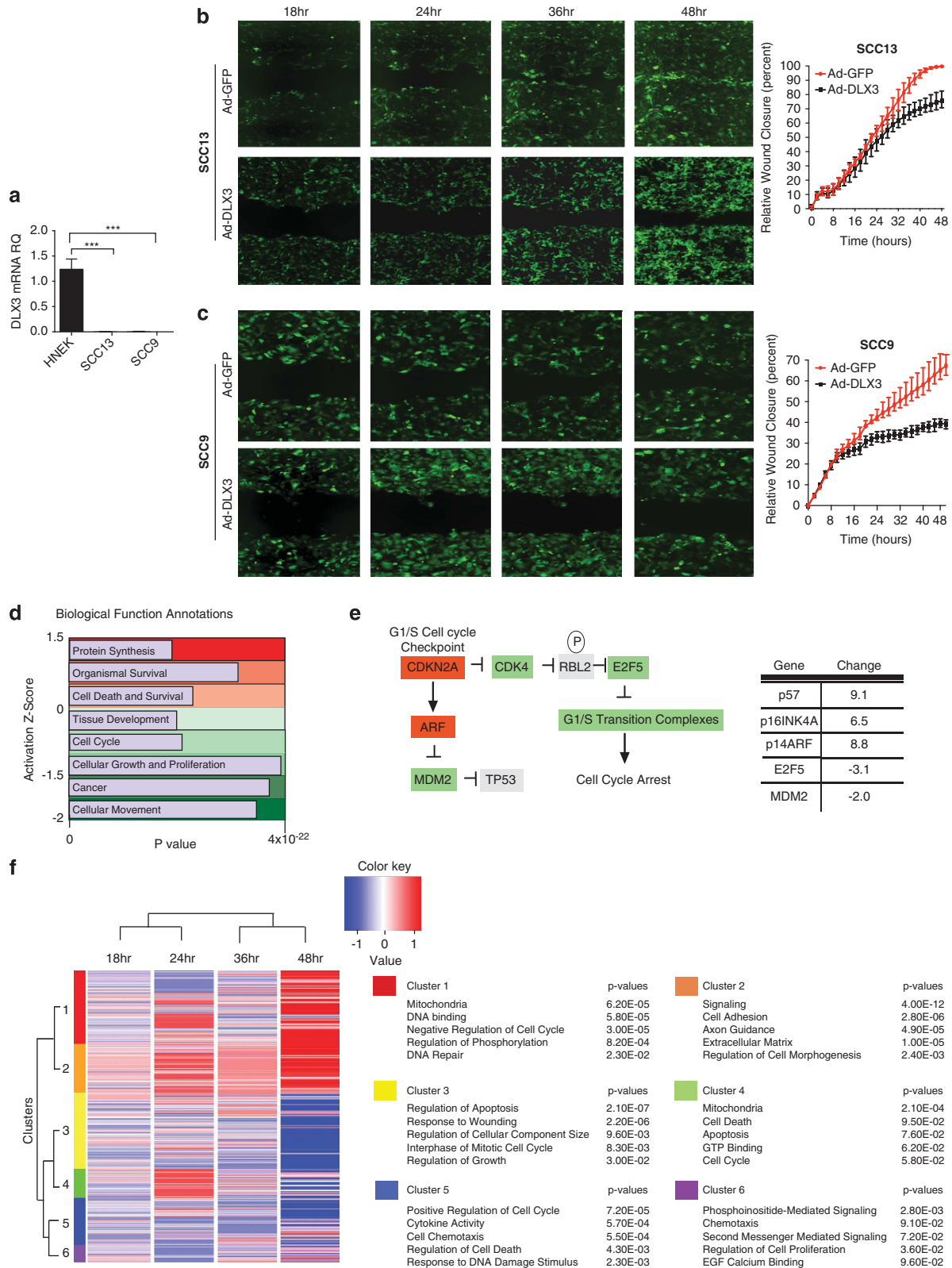


**Figure 5.** DLX3 expression is lost in human squamous carcinoma. (a) Immunohistochemical staining of normal skin, SCC of grade I and II, metastatic adenocarcinoma and undifferentiated carcinoma sections with antibodies against K5 and DLX3. Scale bars, 20  $\mu$ m. (b) Box plots showing DLX3, TP53, KRT1 and TP63 expression levels in oral SCC and normal samples by Oncomine database. (c) Box plots showing DLX3 expression levels in head and neck SCC samples determined by The Cancer Genome Atlas Database. G1–G4 indicate increased severity in tumor stages.



clusters 1 and 2. In clusters 3–6, we observe downregulation of apoptosis regulation, cell cycle and cell chemotaxis with the most pronounced differences at 48 h (Figure 6f). This suggests that DLX3 function may lead to a metabolically active cell cycle arrest in SCC cells through the upregulation of genes involved in

cycle arrest and a downregulation of genes involved in the pro-apoptosis pathway (Supplementary Tables 6 and 7). Thus, our results indicate that the reinstatement of DLX3 is sufficient to attenuate SCC cell migration and affect transcriptional changes involved in signaling, adhesion, cell cycle and cell movement.



Collectively, our results support the emerging concept that DLX3 acts as a key regulator of cell cycle progression and squamous tumor growth.

## DISCUSSION

This work establishes the functional association of the DLX3 within p53-regulated networks in skin keratinocytes and in cutaneous tumorigenesis. Functionally, we show that DLX3 expression is necessary for cell cycle block and differentiation. An integrated transcriptome analysis identified a DLX3-dependent gene signature characterized by downregulation of the DNA replication signaling pathway and upregulation of the p53-dependent cell cycle-related genes.

The p53 network signaling, which includes p63 isoforms ( $\Delta$ Np63 and TAp63) and p21, is determinant in promoting keratinocyte maturation.<sup>28,31,47</sup>

Notably,  $\Delta$ Np63 isoform overexpression is characteristic of SCC and other epithelial cancers<sup>11,13,48,49</sup> and it correlates with decreased differentiation and increased oncogenic activity.<sup>15,43,50,51</sup> Recent work by Chakravarti *et al.*<sup>52</sup> provides a mechanistic understanding on the role of  $\Delta$ Np63 in epidermal differentiation by demonstrating that  $\Delta$ Np63 transcriptionally regulates the miRNA processing cofactor DGCR8 to reprogram adult somatic cells into multipotent stem cells. In contrast, TA isoforms are associated with cell cycle arrest by the transactivation of p53 target genes, such as *p21*, *BAX* or *PERP* and assume the role of tumor suppressors.<sup>34</sup> TAp63 was recently reported to suppress a wide variety of tumors *in vivo* including cutaneous SCC<sup>17</sup> and to transcriptionally regulate p57 to maintain stem cells in the dermis in quiescence using *in vivo* models.<sup>16</sup> Recent work establishes a significant p63–p53 interplay in the differential expression of the transcription factor Runx1 in proliferative or differentiated human keratinocytes. Interestingly, as for  $\Delta$ Np63, RUNX1 expression was strongly expressed in basal cell carcinomas and, in parallel to p53, was downregulated in SCC.<sup>28</sup>

It has been previously reported that exogenous expression of the homeobox transcription factor DLX3 decreases  $\Delta$ Np63 protein levels through proteasomal degradation.<sup>25</sup> Here we report that the loss of DLX3 increases  $\Delta$ Np63 expression and that p63 transcriptional targets, such as NoxA, decrease upon the exogenous expression of DLX3 in keratinocytes. Therefore, DLX3 may be responsible for the reduction of  $\Delta$ Np63 $\alpha$  expression during the differentiation of the stratified epithelia.

We also found that exogenous DLX3 increases the expression of TAp63 and its transcriptional target p57, thus regulating p63 signaling at multiple levels. Furthermore, exogenous DLX3 expression significantly increased p57 levels in v-ras<sup>H1a</sup> keratinocytes and SCC13 cells. Therefore, DLX3 function in the context of transformed cells could induce cell cycle exit through the TAp63–p57 axis.

Here we present evidence that loss of DLX3 removes a proliferative brake from keratinocytes conducive to a pre-neoplastic state with the development of a molecular signature characteristic of tumorigenic SCC cells. In the case of the p53 target p21, the association between p53 and DLX3 within the p21 promoter is directly required to p21 expression. In a

broader sense, our results establish DLX3 and p53 signaling networks as interconnected circuits that regulate epidermal differentiation in normal epidermal keratinocytes.

We demonstrate that DLX3 is lost in human and experimentally induced murine SCCs corroborating a potential tumor suppression function of DLX3 in the context of cutaneous tumorigenesis. Mechanistically, we show that DLX3 expression itself may modulate ERK activation, and the loss of DLX3 is potentially linked to an activated mitogenic phenotype required for the development of neoplastic lesions.

Collectively, our data support the correlation between DLX3 and p53-regulated network in skin tumorigenesis, identifying DLX3 as an essential modulator in the regulation of cell cycle exit and revealing its tumor suppressor activity in epidermal cells. We show that the addition of DLX3 function in SCC lines is sufficient to cause altered migration in a scratch wound assay resulting in decreased wound closure. Molecularly, we demonstrate that DLX3 alone impacts cell cycle exit. We propose that reinstatement of DLX3 function in squamous tumors could potentially be used to reduce tumor growth by restoring responses to a differentiation signal in the skin.

## MATERIALS AND METHODS

### Generation and analysis of mice

Mouse experiments were approved by NIAMS Animal Care and Use Committee. DLX3cKO mice were generated and genotyped as previously reported.<sup>53</sup> The two-stage model of skin carcinogenesis was performed as previously described.<sup>41</sup> For this experiment all animals, male or female, received treatments while untreated skin was used as control. No blind studies were performed.

### Cell culture and transduction

Normal human epidermal keratinocytes (NHEK) were obtained from surgically resected human foreskins from the NIH Clinical Center, Dermatology Branch, after provision of written consent. NHEK were isolated as previously described<sup>54</sup> and maintained in KGM (Lonza, Basel, Switzerland), with Ca<sup>++</sup> concentration of 0.05 mM (proliferating media). To induce human keratinocyte differentiation, a final concentration of 1.8 mM Ca<sup>++</sup> was used. We transduced NHEK with retroviral vectors containing or not DLX3 cDNA (pHan-DLX3/Flag and pHan-EV, respectively) in the presence of 4  $\mu$ g/ml polybrene (Sigma, St Louis, MO, USA). Retroviral particle were generated in Phoenix cells using ProFection Mammalian Transfection Systems kit (Promega, Madison, WI, USA). We monitored morphological changes of transduced cells in culture using a Carl Zeiss AxioVert S100 microscope, AxioCam HRm Carl Zeiss digital camera (Carl Zeiss International, Jena, Germany) and visualized using AxioVision Rel. 4.4 software (Carl Zeiss International). Primary murine keratinocytes were isolated from DLX3cKO and WT mice as previously described.<sup>55</sup> For each experimental replicate, a minimum of 10 newborn mice were used. Primary murine keratinocytes were cultured in supplemented minimal essential medium (Gibco, Thermo Fisher Scientific Inc., Waltham, MA, USA) with 8% fetal bovine serum (FBS, Atlanta Biologicals, Flowery Branch, GA, USA) and 1% antibiotic (Penicillin Streptomycin Amphotericin B, Sigma), with Ca<sup>++</sup> concentration of 0.05 mM. To induce keratinocyte differentiation, a final concentration of 0.12 mM Ca<sup>++</sup> was used. HCT116 cells were cultured in McCoy's 5A media (Gibco, Thermo Fisher Scientific Inc.) supplemented with 10% FBS (Atlanta Biologicals) and 1% antibiotic (Pen-strep, Sigma). SCC13 and SCC9 cells were cultured in DMEM/F12+GlutaMAX+sodium

**Figure 6.** DLX3 attenuates the migration of SCC cells. (a) Relative mRNA expression levels of DLX3 in NHEK, SCC13 and SCC9 (mean  $\pm$  s.d.; \*\*\* $P < 0.001$ ). Scratch wound assay of (b) SCC13 cells and (c) SCC9 cells infected with Ad-GFP or Ad-DLX3 with GFP fluorescent images taken 18, 24, 36 and 48 h after scratch and infection. Right panel: relative wound closure percentage of cells measured every 2 h for 48 h after scratch and infection. (d) Top significant biological function annotations identified by Ingenuity Pathway Analysis of differentially regulated SCC13 mRNA fold changes comparing Ad-DLX3 versus Ad-GFP samples 48 h after infection (fold change  $> 2$  or  $< -2$ ). (e) G1 to S cell cycle control pathway determined by Wikipathways database overlaid with RNA-seq of SCC13 cells infected with Ad-DLX3 compared with Ad-GFP after 48 h of infection. Red and green boxes represent up- and downregulated genes, respectively. Right panel: fold changes of differentially expressed mRNA at 48 h after infection. (f) Heat map of hierarchically clustered fold changes of SCC13 mRNA infected with DLX3 compared with GFP control at 18, 24, 36 and 48 h post infection. Clusters were analyzed by DAVID Bioinformatics Functional Analysis Tool with the top five significant functional annotations listed for each cluster.



pyruvate (Gibco, Thermo Fisher Scientific Inc.) supplemented with 10% FBS (Atlanta Biologicals) and 1% antibiotic (Penicillin Streptomycin Amphotericin B, Sigma).

Cells were transfected with scramble siRNA or p53 siRNA (100 nM, Thermo Scientific, Rockville, MD, USA), or scramble siRNA; transduced with GFP or DLX3 adenoviruses (50 multiplicity of infection; Vector Biolab, Malvern, PA, USA); control or v-ras<sup>Ha</sup> retrovirus (1 multiplicity of infection) in the presence of 4 µg/ml polybrene (Penicillin Streptomycin Amphotericin B, Sigma). Retroviral particles were generated as previously described.<sup>56</sup>

#### Site-directed mutagenesis and luciferase reporter assay

The p21 promoter region (−2475/+1) was ligated into pGL3 basic vector (Promega), and confirmed by restriction digestion and sequencing. Using Quikchange (Stratagene, Santa Clara, CA, USA), we introduced mutations on the DLX3-binding site within the p21<sup>−2475/+1</sup> WT promoter construct. Mutagenesis was confirmed by sequencing. The following primers were used to mutate or delete the DLX3-binding sites: p21WT\_forward: TTTT TTCTCGAGTGTGTGGAGGTGACTTCTCTGAAATCTGA; p21WT\_reverse: TTTTTT AAGCTTTGACCAACTGTGGGAAGGACTAACTCGTTT; p21Del\_forward: TTTTTT TCGAGGGAGGAGGTGACAGCACTCAGCAGTTCAGTTAT; p21Del\_reverse: TTTT TTAAGCTTTGACCAACTGTGGGAAGGACTAACTCGTTT; p21Mut\_forward: GACC CCAGATGGCCAAGGATGTCCCACTTTGC; p21Mut\_reverse: GCAAAGTGGGA CATCCTTGCCATCTGGGGT. Using Dual-Luciferase Reporter Assay System (Promega), lysates from transfected keratinocytes were analyzed using a 20/20<sup>n</sup> Luminometer (Turner Systems, Madison, WI, USA) 48 h after transfection.

#### Electrophoresis mobility shift assay

Electromobility shift assay was performed as previously described.<sup>57</sup> A probe containing the DLX3 consensus-binding site (GGGGGATAATTGCTGG) and a probe containing the DLX3-binding site motif of the p21 promoter (GGGGATAATTAAGGA) were used to perform the assay in presence of the recombinant protein DLX3. For the competition assays, mutated (GGGGATGCGCGCTGG) and WT unlabeled probes were used. To perform the super-shift, the reaction was incubated with 3 µg of anti-DLX3 (Abnova, Walnut, CA, USA; H00001747).

#### Thymidine incorporation proliferation assay

Primary keratinocytes (NHEK and primary murine keratinocytes) were plated in 24-well tissue culture plates and RAS transduced on day 3. Cells were pulsed for 4 h with 1 µCi [<sup>3</sup>H]thymidine (GE Healthcare, Milwaukee, WI, USA). Cells were fixed using methanol and acetic acid (in a 3:1 ratio) and then solubilized in 5 n NaOH. The incorporated counts were measured using a scintillation counter.

#### RNA extraction and quantitative reverse transcription-PCR

Total RNA was extracted using RNeasy kit (Qiagen, Valencia, CA, USA) according to the manufacturer's instructions. cDNA was prepared using the ImProm-II Reverse Transcription System (Promega). For each gene, quantitative reverse transcription-PCR analysis was done in triplicate using the iQSYBR Green Supermix (Bio-Rad, Hercules, CA, USA). The following genes were analyzed: *DLX3*, *p53*, *p21*, *p57*, *ΔNp63*, *TAp63*, *KRT14*, *KRT10* and *Cxcl1*. Primer sequences used in quantitative reverse transcription-PCR as indicated (Supplementary Table 8). Relative expression was normalized against the housekeeping gene RPLPO or β-actin. Fold changes were calculated by the Ct method as described previously.<sup>58</sup>

#### Western blot

Lysates of cells and tissues were prepared in SDS sample buffer (60 mM Tris-HCl at pH 6.8, 10% glycerol, 2% SDS and 5% 2-mercaptoethanol). Equal amounts of proteins (25 µg) were separated on 4–12% SDS-polyacrylamide gel electrophoresis gels, transferred to polyvinylidene difluoride membranes (Invitrogen, Waltham, MA, USA), and incubated with primary antibodies specific to ERK (Cell Signaling; 4695), P-ERK (Cell Signaling, Danvers, MA, USA; 4370S), H-RAS (Santa Cruz, Dallas, TX, USA; sc-520), Krt10 (Covance, Princeton, NJ, USA; PRB-159P) and Vinculin (Sigma; V4139). Blots were rinsed in TBST and incubated in peroxidase-conjugated anti-mouse or anti-rabbit secondary antibodies, respectively. Proteins were visualized using an ECL detection system (Pierce Biotech, Waltham, MA, USA) and exposed to film. All experiments were repeated in triplicate.

#### ChIP

NHEK and primary murine keratinocytes maintained in proliferative or differentiating media, were fixed with formaldehyde and processed using the ChIP Assay Kit (Millipore, Billerica, MA, USA) as per the manufacturer's instructions. The following antibodies were used: anti-IgG (Abcam, Cambridge, MA, USA; ab46540); anti-DLX3 (Abcam; ab66390); anti-H3K4me3 (Diagenode, Denville, NJ, USA; C15410003) and anti-H3K27me3 (Diagenode; C15410195). The following primers were used to amplify p21 promoter region: for mouse: p21 forward: CATGTTCCAGCCTGGAA TTGAAGAG, p21 reverse: ATACAGTACCTGACACATACACACC; for human: p21 forward: CATTCCCCTACCCCATGCTGCTC; p21 reverse: CTCAGGGC TGAAAGGTTT.

#### Flow cytometry

Cells were prepared in 70% ethanol and stained with propidium iodide (20 mg/ml). Data were acquired on BD Biosciences (Franklin Lakes, NJ, USA) FACSCanto and analysis was performed using FlowJo Software (FlowJo, LLC, Ashland, OR, USA).

#### Histology and immunohistochemistry

For histological (hematoxylin and eosin staining) and immunohistochemical analysis, tissues were fixed with 4% paraformaldehyde and embedded in paraffin. The 5-µm sections were prepared for specific staining. Each section was incubated overnight at 4°C with the primary antibodies which included: DLX3 (Epitomics, Burlingame, CA, USA; 8434-1), Krt5 (Acris, Jönköping, Sweden; BP5006) and Krt13 (Abcam; ab92551). The Alexa Fluor 488- and 555-conjugated anti-rabbit antibodies (Thermo Fisher Scientific Inc., Waltham, MA, USA) were used as secondary antibodies.

#### mRNA expression profiling and RNA sequencing

For microarray analysis, the Affymetrix GeneChip Scanner 3000 running Affymetrix (GeneChip Operating Software, Santa Clara, CA, USA) was used. Significantly affected genes ( $P < 0.05$  and fold change  $> 1.5$ ) were determined on analysis of variance. RNA from SCC13 cells infected with Ad-GFP or Ad-DLX3 was extracted with Trizol (Life Technologies, Carlsbad, CA, USA). RNA-seq was performed as previously described.<sup>59</sup> mRNA expression profiling were performed in the NIAMS Genome Core Facility at the NIH. Reads were mapped to the human genome using TopHat software (<http://tophat.cbcb.umd.edu>). Expression values (reads per kilobase of transcript per million mapped reads (r.p.k.m.)) and fold changes were calculated and analyzed with the Partek Genomics Suite (<http://www.partek.com>) and analysis of variance statistics. Genes with robust expression (r.p.k.m.  $> 1$ ) were considered for further analysis. The row clustering for the heat map was clustered using Pearson correlation across all samples. The heat map values represent the log<sub>2</sub> fold change ( $> 1 = > 2$  fold up and  $< -1 = < -2$  fold down). Analysis of clusters was done using DAVID Bioinformatics Functional Annotation Tool (<http://david.abcc.ncifcrf.gov/summary.jsp>). Completed microarray and RNA-seq data have been deposited in the Gene Expression Omnibus (GSE63049) site.

#### Human skin and SCC

Human skin and SCC samples were from Biomax SCC tissue array (US Biomax, Rockville, MD, USA; Cat#: sk-208), that contained 60 cases of skin cancer (SCC and metastatic adenocarcinoma) plus 9 cases of normal tissue from autopsy. Squamous tumor and adenocarcinoma are ranked from grade 1–4 as pathological diagnosis, which is equivalent to well differentiated, moderately differentiated, poorly differentiated or undifferentiated, respectively. Pathological grade was confirmed for all cases.

#### Scratch wound assay

A total of  $2 \times 10^4$  cells of SCC13 and SCC9 cells were seeded in 96-well ImageLock plates (ESSEN BioScience, Ann Arbor, MI, USA) and grown to 90–95% confluency. Subsequently, a scratch was placed in the middle of the wells with the WoundMaker (ESSEN BioScience). After washing with phosphate-buffered saline, the respective virus (Ad-GFP or Ad-DLX-GFP at a titer of  $10^{10}$  plaque-forming units) was added to each well at a multiplicity of infection of 50. The cells were grown in DMEM/F12 +GlutaMAX+sodium pyruvate (Gibco, Thermo Fisher Scientific Inc.) supplemented with 5% bovine serum albumin. Pictures were taken every 2 h for 48 h using the IncuCyte ZOOM 40008 instrument and analyzed with the IncuCyte Zoom 2013A software (ESSEN BioScience).

## Computational analysis

Microarray expression fold changes were calculated using Partek Genomics Suite (<http://www.partek.com>). Pathway enrichment was calculated using the hypergeometric distribution and WikiPathways.<sup>60</sup> All heat maps were generated with the R programming environment using Wards method with Euclidean distance (<http://www.r-project.org/>). Cytoscape was used for network visualization.<sup>61</sup>

## Statistical analysis

For all experiments *in vitro* technical and biological triplicates were performed. The data were analyzed by Prism Software (GraphPad Software, La Jolla, CA, USA) and significance values were assessed by the Student's *t*-test. For all experiments with error bars, s.d.'s were calculated to indicate variations within each experiment and data, and values represent mean  $\pm$  s.d. of mean.  $P < 0.05$ ,  $P < 0.01$  and  $P < 0.001$  were considered significant.

## CONFLICT OF INTEREST

The authors declare no conflict of interest.

## ACKNOWLEDGEMENTS

We thank current and past members of the Laboratory of Skin Biology and members of the Laboratory of Cancer Biology and Genetics, and Dr Mark Udey for helpful discussions. We also thank Andrew Ryscavage (LCBG), Gustavo Gutierrez-Cruz (NIAMS Genome Analysis Core Facility), Dr Hong-Wei Sun (Biodata Mining and Discovery Section, NIAMS) and Kristina Zaal of the NIAMS Light Imaging Core Facility. This work was supported by the Intramural Research Program of the National Institute of Arthritis and Musculoskeletal and Skin Diseases of the National Institutes of Health (M.I.M.ZIA AR041124-14).

## REFERENCES

- 1 Karia PS, Han J, Schmults CD. Cutaneous squamous cell carcinoma: estimated incidence of disease, nodal metastasis, and deaths from disease in the United States, 2012. *J Am Acad Dermatol* 2013; **68**: 957–966.
- 2 Ratushny V, Gober MD, Hick R, Ridky TW, Seykora JT. From keratinocyte to cancer: the pathogenesis and modeling of cutaneous squamous cell carcinoma. *J Clin Invest* 2012; **122**: 464–472.
- 3 Hodis E, Watson IR, Kryukov GV, Arold ST, Imielinski M, Theurillat JP *et al*. A landscape of driver mutations in melanoma. *Cell* 2012; **150**: 251–263.
- 4 Levine AJ, Hu W, Feng Z. The P53 pathway: what questions remain to be explored? *Cell Death Differ* 2006; **13**: 1027–1036.
- 5 Petitjean A, Achatz MI, Borresen-Dale AL, Hainaut P, Olivier M. TP53 mutations in human cancers: functional selection and impact on cancer prognosis and outcomes. *Oncogene* 2007; **26**: 2157–2165.
- 6 Radoja N, Gazel A, Banno T, Yano S, Blumenberg M. Transcriptional profiling of epidermal differentiation. *Physiol Genomics* 2006; **27**: 65–78.
- 7 Missero C, Di Cunto F, Kiyokawa H, Koff A, Dotto GP. The absence of p21Cip1/WAF1 alters keratinocyte growth and differentiation and promotes ras-tumor progression. *Genes Dev* 1996; **10**: 3065–3075.
- 8 Taylor WR, Stark GR. Regulation of the G2/M transition by p53. *Oncogene* 2001; **20**: 1803–1815.
- 9 Botchkarev VA, Flores ER. p53/p63/p73 in the epidermis in health and disease. *Cold Spring Harb Perspect Med* 2014; **4**: 1–12.
- 10 Morasso MI, Radoja N. Dlx genes, p63, and ectodermal dysplasias. *Birth Defects Res C Embryo Today* 2005; **75**: 163–171.
- 11 Su X, Chakravarti D, Flores ER. p63 steps into the limelight: crucial roles in the suppression of tumorigenesis and metastasis. *Nat Rev Cancer* 2013; **13**: 136–143.
- 12 Crum CP, McKeon FD. p63 in epithelial survival, germ cell surveillance, and neoplasia. *Annu Rev Pathol* 2010; **5**: 349–371.
- 13 King KE, Ha L, Camilli T, Weinberg WC. Delineating molecular mechanisms of squamous tissue homeostasis and neoplasia: focus on p63. *J Skin Cancer* 2013; **2013**: 632028.
- 14 Dotto JE, Glusac EJ. p63 is a useful marker for cutaneous spindle cell squamous cell carcinoma. *J Cutan Pathol* 2006; **33**: 413–417.
- 15 Romano RA, Smalley K, Magraw C, Serna VA, Kurita T, Raghavan S *et al*. DeltaNp63 knockout mice reveal its indispensable role as a master regulator of epithelial development and differentiation. *Development* 2012; **139**: 772–782.
- 16 Su X, Paris M, Gi YJ, Tsai KY, Cho MS, Lin YL *et al*. TAp63 prevents premature aging by promoting adult stem cell maintenance. *Cell Stem Cell* 2009; **5**: 64–75.

- 17 Su X, Chakravarti D, Cho MS, Liu L, Gi YJ, Lin YL *et al*. TAp63 suppresses metastasis through coordinate regulation of Dicer and miRNAs. *Nature* 2010; **467**: 986–990.
- 18 Duverger O, Morasso MI. Role of homeobox genes in the patterning, specification, and differentiation of ectodermal appendages in mammals. *J Cell Physiol* 2008; **216**: 337–346.
- 19 Abate-Shen C. Deregulated homeobox gene expression in cancer: cause or consequence? *Nat Rev Cancer* 2002; **2**: 777–785.
- 20 Paik JH, Kollipara R, Chu G, Ji H, Xiao Y, Ding Z *et al*. FoxOs are lineage-restricted redundant tumor suppressors and regulate endothelial cell homeostasis. *Cell* 2007; **128**: 309–323.
- 21 Morasso MI, Markova NG, Sargent TD. Regulation of epidermal differentiation by a Distal-less homeodomain gene. *J Cell Biol* 1996; **135**: 1879–1887.
- 22 Park GT, Morasso MI. Regulation of the Dlx3 homeobox gene upon differentiation of mouse keratinocytes. *J Biol Chem* 1999; **274**: 26599–26608.
- 23 Hwang J, Kita R, Kwon HS, Choi EH, Lee SH, Udey MC *et al*. Epidermal ablation of Dlx3 is linked to IL-17-associated skin inflammation. *Proc Natl Acad Sci USA* 2011; **108**: 11566–11571.
- 24 Priolo M, Lagana C. Ectodermal dysplasias: a new clinical-genetic classification. *J Med Genet* 2001; **38**: 579–585.
- 25 Di Costanzo A, Festa L, Duverger O, Vivo M, Guerrini L, La Mantia G *et al*. Homeodomain protein Dlx3 induces phosphorylation-dependent p63 degradation. *Cell Cycle* 2009; **8**: 1185–1195.
- 26 Radoja N, Guerrini L, Lo Iacono N, Merlo GR, Costanzo A, Weinberg WC *et al*. Homeobox gene Dlx3 is regulated by p63 during ectoderm development: relevance in the pathogenesis of ectodermal dysplasias. *Development* 2007; **134**: 13–18.
- 27 Vanbokhoven H, Melino G, Candi E, Declercq W. p63, a story of mice and men. *J Invest Dermatol* 2011; **131**: 1196–1207.
- 28 Masse I, Barbolat-Boutrand L, Molina M, Berthier-Vergnes O, Joly-Tonetti N, Martin MT *et al*. Functional interplay between p63 and p53 controls RUNX1 function in the transition from proliferation to differentiation in human keratinocytes. *Cell Death Dis* 2012; **3**: e318.
- 29 Sherr CJ, Roberts JM. CDK inhibitors: positive and negative regulators of G1-phase progression. *Genes Dev* 1999; **13**: 1501–1512.
- 30 Topley GI, Okuyama R, Gonzales JG, Conti C, Dotto GP. p21(WAF1/Cip1) functions as a suppressor of malignant skin tumor formation and a determinant of keratinocyte stem-cell potential. *Proc Natl Acad Sci USA* 1999; **96**: 9089–9094.
- 31 Candi E, Agostini M, Melino G, Bernassola F. How the TP53 family proteins TP63 and TP73 contribute to tumorigenesis: regulators and effectors. *Hum Mutat* 2014; **35**: 702–714.
- 32 Gandarillas A. The mysterious human epidermal cell cycle, or an oncogene-induced differentiation checkpoint. *Cell Cycle* 2012; **11**: 4507–4516.
- 33 Candi E, Rufini A, Terrinoni A, Giamboni-Miraglia A, Lena AM, Mantovani R *et al*. DeltaNp63 regulates thymic development through enhanced expression of FgfR2 and Jag2. *Proc Natl Acad Sci USA* 2007; **104**: 11999–12004.
- 34 Guo X, Keyes WM, Papazoglu C, Zuber J, Li W, Lowe SW *et al*. TAp63 induces senescence and suppresses tumorigenesis in vivo. *Nat Cell Biol* 2009; **11**: 1451–1457.
- 35 Koster MI, Roop DR. p63 and epithelial appendage development. *Differentiation* 2004; **72**: 364–370.
- 36 Koh LF, Ng BK, Bertrand J, Thierry F. Transcriptional control of late differentiation in human keratinocytes by TAp63 and Notch. *Exp Dermatol* 2015; **24**: 754–760.
- 37 Schavolt KL, Pietenpol JA. p53 and Delta Np63 alpha differentially bind and regulate target genes involved in cell cycle arrest, DNA repair and apoptosis. *Oncogene* 2007; **26**: 6125–6132.
- 38 Wei CL, Wu Q, Vega VB, Chiu KP, Ng P, Zhang T *et al*. A global map of p53 transcription-factor binding sites in the human genome. *Cell* 2006; **124**: 207–219.
- 39 Bunz F, Dutriaux A, Lengauer C, Waldman T, Zhou S, Brown JP *et al*. Requirement for p53 and p21 to sustain G2 arrest after DNA damage. *Science* 1998; **282**: 1497–1501.
- 40 Saramaki A, Banwell CM, Campbell MJ, Carlberg C. Regulation of the human p21(waf1/cip1) gene promoter via multiple binding sites for p53 and the vitamin D3 receptor. *Nucleic Acids Res* 2006; **34**: 543–554.
- 41 Darwiche N, Ryscavage A, Perez-Lorenzo R, Wright L, Bae DS, Hennings H *et al*. Expression profile of skin papillomas with high cancer risk displays a unique genetic signature that clusters with squamous cell carcinomas and predicts risk for malignant conversion. *Oncogene* 2007; **26**: 6885–6895.
- 42 Roop DR, Lowy DR, Tambourin PE, Strickland J, Harper JR, Balaschak M *et al*. An activated Harvey ras oncogene produces benign tumours on mouse epidermal tissue. *Nature* 1986; **323**: 822–824.
- 43 Ha L, Ponnampertuma RM, Jay S, Ricci MS, Weinberg WC. Dysregulated DeltaNp63alpha inhibits expression of Ink4a/arf, blocks senescence, and promotes malignant conversion of keratinocytes. *PLoS One* 2011; **6**: e21877.

- 44 Tu Z, Aird KM, Zhang R. RAS, cellular senescence and transformation: the BRCA1 DNA repair pathway at the crossroads. *Small GTPases* 2012; **3**: 163–167.
- 45 Cataisson C, Ohman R, Patel G, Pearson A, Tsien M, Jay S *et al*. Inducible cutaneous inflammation reveals a protumorigenic role for keratinocyte CXCR2 in skin carcinogenesis. *Cancer Res* 2009; **69**: 319–328.
- 46 Burns JE, Baird MC, Clark LJ, Burns PA, Edington K, Chapman C *et al*. Gene mutations and increased levels of p53 protein in human squamous cell carcinomas and their cell lines. *Br J Cancer* 1993; **67**: 1274–1284.
- 47 Cai BH, Chao CF, Lu MH, Lin HC, Chen JY. A half-site of the p53-binding site on the keratin 14 promoter is specifically activated by p63. *J Biochem* 2012; **152**: 99–110.
- 48 Flores ER. The roles of p63 in cancer. *Cell Cycle* 2007; **6**: 300–304.
- 49 King KE, Weinberg WC. p63: defining roles in morphogenesis, homeostasis, and neoplasia of the epidermis. *Mol Carcinog* 2007; **46**: 716–724.
- 50 Rocco JW, Leong CO, Kuperwasser N, DeYoung MP, Ellisen LW. p63 mediates survival in squamous cell carcinoma by suppression of p73-dependent apoptosis. *Cancer Cell* 2006; **9**: 45–56.
- 51 Senoo M, Pinto F, Crum CP, McKeon F. p63 is essential for the proliferative potential of stem cells in stratified epithelia. *Cell* 2007; **129**: 523–536.
- 52 Chakravarti D, Su X, Cho MS, Bui NH, Coarfa C, Venkatanarayan A *et al*. Induced multipotency in adult keratinocytes through down-regulation of DeltaNp63 or DGCR8. *Proc Natl Acad Sci USA* 2014; **111**: E572–E581.
- 53 Hwang J, Mehrani T, Millar SE, Morasso MI. Dlx3 is a crucial regulator of hair follicle differentiation and cycling. *Development* 2008; **135**: 3149–3159.
- 54 Aasen T, Izpisua Belmonte JC. Isolation and cultivation of human keratinocytes from skin or plucked hair for the generation of induced pluripotent stem cells. *Nat Protoc* 2010; **5**: 371–382.
- 55 Lichti U, Anders J, Yuspa SH. Isolation and short-term culture of primary keratinocytes, hair follicle populations and dermal cells from newborn mice and keratinocytes from adult mice for in vitro analysis and for grafting to immunodeficient mice. *Nat Protoc* 2008; **3**: 799–810.
- 56 Cataisson C, Salcedo R, Hakim S, Moffitt BA, Wright L, Yi M *et al*. IL-1R-MyD88 signaling in keratinocyte transformation and carcinogenesis. *J Exp Med* 2012; **209**: 1689–1702.
- 57 Duverger O, Lee D, Hassan MQ, Chen SX, Jaisser F, Lian JB *et al*. Molecular consequences of a frameshifted DLX3 mutant leading to Tricho-Dento-Osseous syndrome. *J Biol Chem* 2008; **283**: 20198–20208.
- 58 Livak KJ, Schmittgen TD. Analysis of relative gene expression data using real-time quantitative PCR and the 2(-Delta Delta C(T)) Method. *Methods* 2001; **25**: 402–408.
- 59 Lessard JC, Kalinin A, Bible PW, Morasso MI. Calmodulin 4 is dispensable for epidermal barrier formation and wound healing in mice. *Exp Dermatol* 2015; **24**: 55–57.
- 60 Kelder T, van Iersel MP, Hanspers K, Kutmon M, Conklin BR, Evelo CT *et al*. Wiki-Pathways: building research communities on biological pathways. *Nucleic Acids Res* 2012; **40**: D1301–D1307.
- 61 Smoot ME, Ono K, Ruscheinski J, Wang PL, Ideker T. Cytoscape 2.8: new features for data integration and network visualization. *Bioinformatics* 2011; **27**: 431–432.

Supplementary Information accompanies this paper on the Oncogene website (<http://www.nature.com/onc>)